

Fueling Pellet Injection in LHD and Its Prospect to Steady State Operation

SAKAMOTO Ryuichi*, YAMADA Hiroshi, KATO Shinji, TANAKA Kenji, SAKAKIBARA Satoru, NARIHARA Kazumichi, MORITA Shigeru, SUZUKI Hajime, INAGAKI Shigeru, OSAKABE Masaki, KANEKO Osamu, KOMORI Akio, SUDO Shigeru, MOTOJIMA Osamu and LHD Experimental Group

National Institute for Fusion Science, Toki, Gifu 509-5292, Japan

(Received: 18 January 2000 / Accepted: 19 May 2000)

Abstract

In the LHD experiment, pellet injection is placed as a fundamental tool since deterioration of fueling efficiency by gas puffing is concerned. The fueling pellet injector, which is developed for LHD with five independent barrels, has demonstrated high reliability and reproducibility.

Pellet injection has extended an operational region of NBI plasmas in LHD to higher densities without confinement deterioration. Several important data, such as plasma stored energy (0.88 MJ), energy confinement time (0.3 s), β (2.4% at 1.3 T) and density ($1.1 \times 10^{20} \text{ m}^{-3}$) were attained by pellet injection.

Particle transport has been analyzed for the near-term LHD experiments using repetitive pellet injection. The analysis suggests that there is prospect of core fueling by repeating pellet injection without perturbation at center.

Keywords:

fueling, particle control, hydrogen pellet, ablation

1. Introduction

Through the study of inter-machine scalings of energy confinement time [1,2], confinement in currentless helical plasma has been proved to be comparable to L-mode in tokamaks while preferable dependence on electron density is more pronounced than in tokamaks. The international stellarator scaling 95 (ISS95) is described as follows.

$$\tau_E^{\text{ISS95}} = 0.08 a_P^{2.21} R_0^{0.65} P_{\text{abs}}^{-0.59} \bar{n}_e^{0.51} B_0^{0.83} \epsilon_{2/3}^{0.40}.$$

Particle control, or fueling and pumping are one of the important issue in research of magnetic confinement fusion. Gas puff fueling has been using widely to build up and sustain plasma density, however fueling

efficiency of gas puffing is not good in large-scale, high-temperature and steady state plasmas since the neutral gas from gas puffing is ionized at the plasma surface. Especially gas puffing is not efficient in LHD, because core plasma region is surrounded with thick ergodic layer that connects to the divertor.

Hydrogen ice pellet injection is one of the important techniques used for core plasma fueling. A fueling pellet injector, which equips independent 5 barrels, has been designed and it has been installed on LHD [3]. The main aim of the present study is to investigate the validity of the pellet fueling and the pellet ablation behavior in LHD.

*Corresponding author's e-mail: sakamoto@LHD.nifs.ac.jp

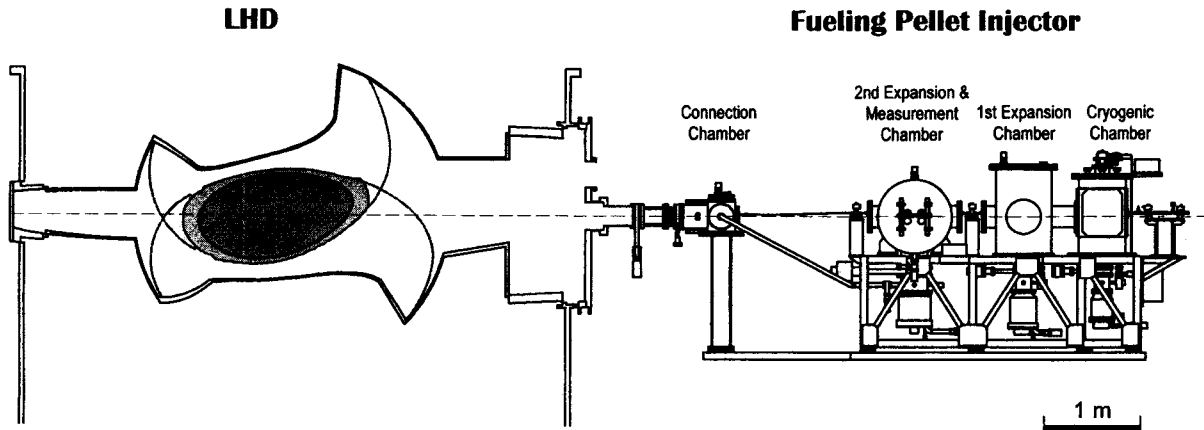


Fig. 1 Schematic drawing of the fueling pellet injector and plasma vacuum vessel of LHD.

2. Experimental Set-up

Figure 1 shows the schematic drawing of the pellet injector and plasma vacuum vessel of LHD. The pellet injector has been connected to the outer port (3-O). The pellet injector uses a pneumatic pipe-gun type barrel, therefore high-pressure helium gas is employed for pellet acceleration. In order to prevent helium gas flow into LHD vacuum vessel, double expansion chambers with large capacity vacuum pumps and fast shutter valves were installed. The size and velocity of the pellet are $3 \text{ mm}\phi \times 3 \text{ mm}l$ and 1 km/s , respectively. The pellet is injected from outer side equator of LHD. Pellet mass was measured by microwave cavity mass detector, and pellet velocity was measured by time of flight method. The injected pellet was checked by shadow graph, which consists of first flash lamp (70 ns) and CCD camera, at an exit of the injector.

Pellet ablation and penetration are measured by first photo diode (500 kHz sampling) and CCD camera (each 33 ms exposure) with $H\alpha$ filter.

3. Pellet Injection into NBI Heated Plasma

Waveform of a typical discharge of pellet injected plasma (#15440, $B_t = 2.75 \text{ T}$, $R_{ax} = 3.6 \text{ m}$, $P_{NBI} = 4 \text{ MW}$) are shown in Fig. 2. Pellet injection is carried out at 0.8, 0.88, 0.96, 1.04 and 1.12 s. Line averaged electron density \bar{n}_e increases sharply at the timing of injection and then increase rate of the plasma stored energy W_p becomes much steeper. Figure 3 shows the dependence of the plasma stored energy on the line averaged electron density. At the timing of injection, the pellet ablates adiabatically, thereby the density increase without change of plasma stored energy, and then the stored energy increases along with recovery of electron

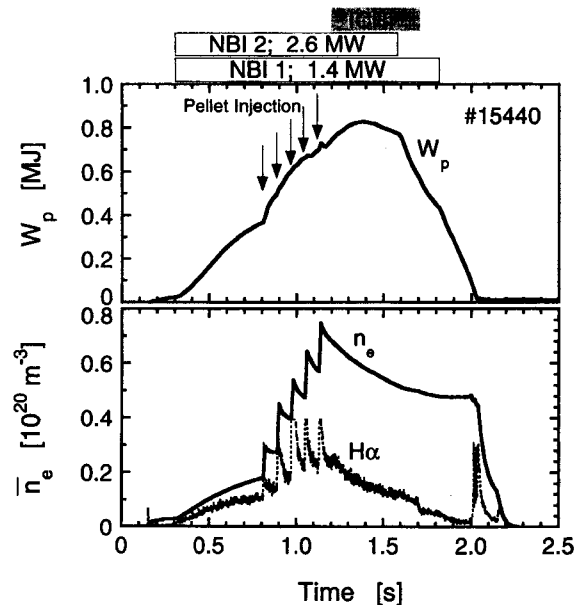


Fig. 2 Typical discharge of pellet injected plasma. Pellet injection is carried out at 0.8, 0.88, 0.96, 1.04 and 1.12 s. (#15440, $B_t = 2.75 \text{ T}$, $R_{ax} = 3.6 \text{ m}$, $P_{NBI} = 4 \text{ MW}$)

temperature.

Figure 4 shows plot of the maximum stored energy versus the density when the stored energy achieved to maximum. Open circles and close circles are data of gas puffing and pellet injection, respectively. The dashed line indicates the stored energy predicted by 1.5 times the international stellarator scaling 95 (ISS95) for a heating power of 4 MW. In the case of gas puffing, the maximum density is $0.5 \times 10^{20} \text{ m}^{-3}$ and the confinement deterioration is observed at density above 0.35×10^{20}

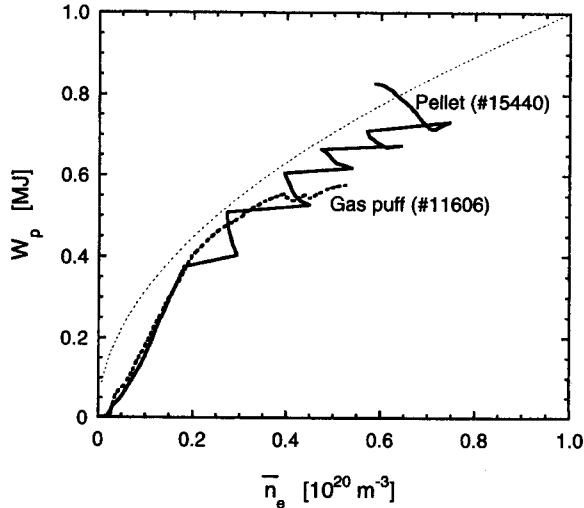


Fig. 3 Stored energy W_p evolution as a function of line averaged electron density \bar{n}_e . Dashed line and solid line shows data of gas puffing and pellet injection, respectively. The dashed line indicates the stored energy predicted by 1.5 times the international stellarator scaling 95 (ISS95) for a heating power of 4 MW.

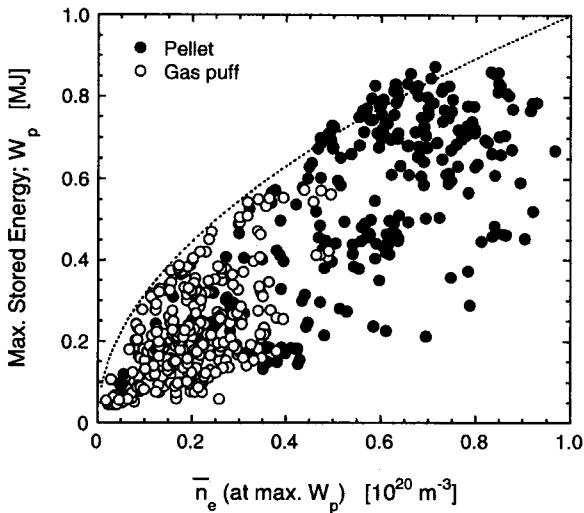


Fig. 4 Maximum plasma stored energy as a function of line averaged electron density. Open circles and close circles show data of gas puffing and pellet injection, respectively.

m^{-3} . In the case of pellet injection, there is no confinement deterioration up to $0.8 \times 10^{20} m^{-3}$, and the stored energy attains to 0.875 MJ. The maximum density achieved is $1.1 \times 10^{20} m^{-3}$. However, the stored energy is saturated at density above $0.8 \times 10^{20} m^{-3}$ for lack of heating power.

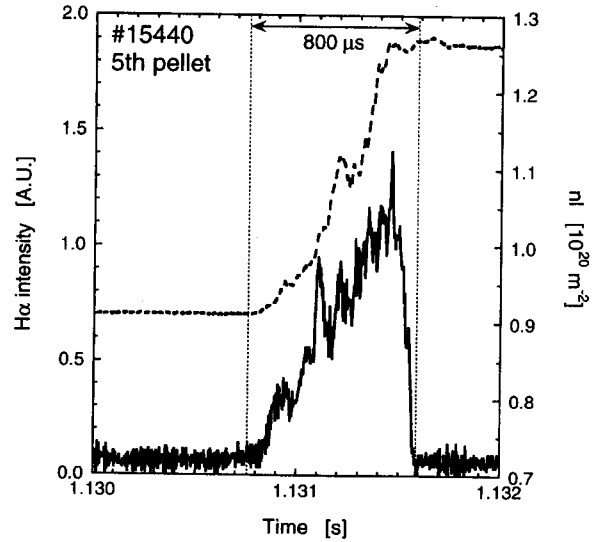


Fig. 5 Temporal evolution of $H\alpha$ light emission from ablating pellet and line density n_l .

4. Ablation

Figure 5 shows the temporal evolution of $H\alpha$ light emission from ablating pellet and line density. $H\alpha$ light emission is consistent with density increase in detail structure. CCD image shows that the trajectory of the $H\alpha$ light emission is straight, therefore time trace of the $H\alpha$ light emission shows the spatial penetration depth on the assumption that velocity of the pellet is constant during the ablation. In this case, the penetration depth is about 0.8 m.

Neutral gas shielding (NGS) model [4], which is simple and the most widely adopted ablation model, can be expressed as follows [5],

$$\lambda/\alpha = CT_e^{-5/9} n_e^{-1/9} m_p^{5/27} v_p^{1/3},$$

where T_e , n_e , m_p , v_p is the central electron temperature, the central electron density, the pellet mass and the pellet velocity, respectively. The scaling suggests that the penetration depth depends mainly on the electron temperature. Triangle symbols in Figure 6 show the comparison of measured penetration depth with prediction from the NGS expression. The measured penetration depth is systematically smaller than NGS model. Regression analysis for ablation database of LHD has been carried out (Open circles in Fig. 6). The result is as follows,

$$\lambda/\alpha = 0.123T_e^{-0.85} n_e^{-0.07} m_p^{0.24} v_p^{0.24}.$$

The penetration depth has pronounced undesirable dependence on the temperature in comparison with NGS.

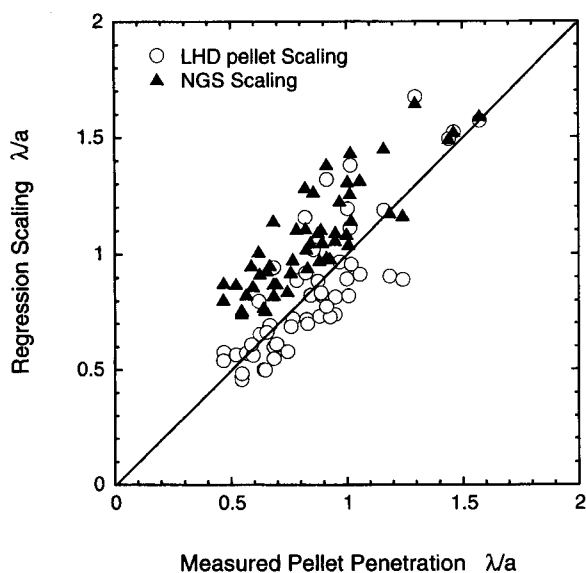


Fig. 6 Comparison of measured penetration depth with predicted penetration depth.

5. Density Sustainment Simulation by Repetitive Pellet Injection

Particle transport has been analyzed for the near-term LHD experiments using repetitive pellet injection. 1-D particle balance is modeled in the three regions, which are plasma, scrape-off layer and vacuum. Figure 7 shows the temporal behavior of densities at the center and in the intermediate radius ($\rho = 0.7$). Temperature profiles are fixed and assumed to be constant in time. When pellets with the diameter of 2.6 mm are injected every 0.2 s with the velocity of 1 km, the central density is kept constant at $5 \times 10^{19} \text{ m}^{-3}$ without any gas puffing and is not perturbed by pellet injection. The pellet is ablated completely outside of $\rho = 0.6$. Although the largest perturbation seen at $\rho = 0.7$ reaches 30%, perturbation in the core region inside $\rho = 0.5$ can be suppressed to less than 10%.

6. Conclusion

Pellet injection has extended operational region of LHD to high density plasma with increased plasma

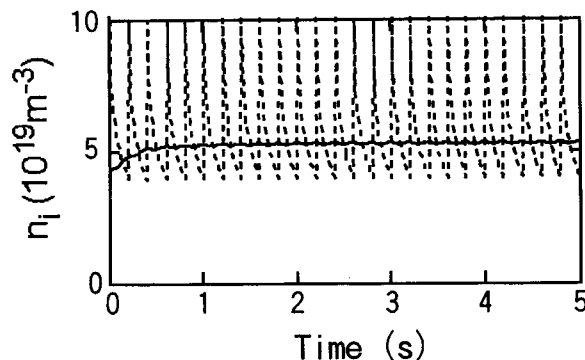


Fig. 7 Temporal behavior of densities at center $\rho = 0$ in a solid line and $\rho = 0.7$ in a dashed line.

stored energy and energy confinement time. Several important data, such as plasma stored energy, energy confinement time, β and density were attained by pellet injection. The maximum electron density attained to $1.1 \times 10^{20} \text{ m}^{-3}$ transiently, the value is twice the maximum density of gas puff fueling plasma. The maximum plasma stored energy attained to 0.875 MJ with 3.6 MW NBI, 0.8 MW ICRF and pellet injection.

In LHD, pellet ablation process and density increase is consistent with each other, but measured penetration depth is smaller than the theory (NGS). The regression analysis shows that the dependence of the penetration depth on the electron temperature is the -0.85 th power. This exponent is 1.5 times larger than NGS prediction ($-5/9$).

The particle transport analysis, which is combined with pellet ablation code, suggests that there is prospect of core fueling by repeating pellet injection without perturbation at center.

Reference

- [1] U. Stroth *et al.*, Nucl. Fusion, **36**, 1063 (1996).
- [2] S. Sudo *et al.*, Nucl. Fusion, **30**, 11 (1990).
- [3] H. Yamada *et al.*, (ISFNT-5).
- [4] P.B. Parks *et al.*, Nucl. Fusion, **17**, 539 (1977).
- [5] L.R. Baylor *et al.*, Nucl. Fusion, **37**, 445 (1997).